

Computer-Assisted Quantitative Evaluation of Coronary Stent Platforms by Different Intracoronary Imaging Methods

E Pociask^{1,2}, K Proniewska^{1,2}, N Bruining¹

¹Erasmus MC, Rotterdam, Netherlands

²AGH University of Science and Technology, Krakow, Poland

Abstract

IVUS (intravascular ultrasound) and OCT (optical coherent tomography) both modalities are used for in-depth analysis in order to provide a detailed description of the anatomy of coronary artery wall and implanted stent positions. Dedicated, semi-automated visualization for both methods was applied. An adaptable quantification algorithm of stent struts detection for OCT and manual quantification of stent struts for IVUS in a series of drug-eluting stented animal coronary arteries were used. The goal of this research was to find significant details and quantitative differences, of implanted coronary stents in both OCT and IVUS intracoronary imaging methods.

1. Introduction

The implantation of intracoronary stents is a standard treatment of coronary atherosclerotic disease. However neoatherosclerosis after stent implantation remains the main problem in interventional cardiology [1]. The in-stent restenosis (ISR) process is very complex and depends on many factors both biological (individual) and technical such as stent fracture or geometry. In order to improve the healing process it is very important to know the behaviour of different stent types [2]. Available technologies are intensively developing in this domain to reduce problems of re-narrowing stented segments.

IVUS is an ultrasound-based intravascular imaging modality that can be used to obtain information about the anatomy of the artery wall, whilst OCT uses light to achieve the same goal. These two imaging methods are based on different physical phenomena, hence have different spatial resolutions, specifically OCT images have a much higher resolution than IVUS. The exact nature and impact of these variation onto quantitative analysis is not yet fully understood. This study investigates the differences of quantitative derived implanted stent parameters by manual and automated detection of stent struts.

2. Methods and materials

Data were acquired from 6 stented coronary pig arteries. First measurements were performed just after drug-stent eluting implantation and second time after 1 year follow up. In summary 24 pullbacks were collected using two different intracoronary imaging techniques: Fourier-Domain OCT (FD-OCT) system (C7 System; LightLab Imaging, Inc/St Jude Medical) and Boston Scientific IVUS iLab (iLab® Ultrasound Imaging System). Every analyzed vessel had implanted drug-eluting stents 3,0 mm in diameter and 16,0 mm in length. All IVUS and OCT analysis were performed using Vessel Analysis software (CURAD BV, Amsterdam, The Netherlands).

2.1. Manual detection of implanted stent struts in IVUS

During recording a pullback rotated IVUS catheter emits ultrasound signal and collects the reflected ultrasound wave which subsequently is converted to a backscattered signal by the transducer [2, 3]. This way longitudinal views of vessels divided into slices are obtained (cross-sectional view) which show the catheter at the center surrounded by the vessel wall [4]. IVUS in itself enables tissue characterization which is based on a visual assessment of gray-scale images. The main focus in this project was the appearance of metal stent struts, which reflect ultrasound beam and appears as bright spots on the images [2].

Pullbacks from first post-implanted cohort and second follow-up cohort were uploaded to the software (Vessel Analysis, CURAD BV, Amsterdam, The Netherlands). Next an expert set the Region of Interest (ROI) with visible stent struts, followed by outlining the lumen, stent and media contours. Stent contours were drawn behind the stent struts and each detected stent strut was assigned manually, and counted by CURAD software.

2.2. Automated detection of implanted stent struts in OCT

OCT is a light-based imaging modality. This technique measures the intensity of back-reflected infra-red light to provide images in similar way as IVUS.

Metal stents struts appear on the images as bright spots with a shadow trail [4-7].

OCT provides high resolution images, allowing visualization of hundreds of stent struts per pullback [4]. Detection and counting of stents struts is time consuming, therefore this study was supported by a computer-assisted stent struts detection algorithm implemented in CURAD software.

The stent detection algorithm searches for isolated regions of maximum intensity in radial profiles. An alternative method additionally selects shadowed regions in the angular distribution. Both methods can be tuned independently with configurable global parameters for maximum performance depending on the properties of the dataset, like enhanced shadowing in post-implant data. The search area is limited to a configurable region around the luminal contour.

Radial distances from detected stent struts to the luminal boundary are calculated automatically for subsequent scoring and statistical processing of user-defined stent-strut classifications. Classes can be defined based on distances only, or combined with manually selected qualitative objectives.

3. Validation of automated detection of stent struts in OCT

Each pullback from both post implanted and follow-up cohort were loaded and like in IVUS procedure, expert set the regions of interest with visible stent struts. Lumen contours detection was performed automatically in CURAD.

3.1. Auto detection parameters

Auto detection parameters were set relative to the lumen border. Therefore correct detection of lumen contours is crucial.

First parameter taken into account, Shadow Trace, had values ranging from -1 to 9 and expert marked a search shadow distance from stent struts by settings minimal and maximal value. Second parameter, Stent Search Area, was used to assign the search area of stent struts and had values from the range of -1 to 9. The last parameter, namely Intensity of struts was selected from range 1 to 10, where 1 means highest brightness of struts. Process of selecting settings for all of those parameters was simultaneously reviewed in the entire pullback by the expert. Table 1 and 2 summarize the collected values of auto detection parameters in post-implanted and follow-up cohorts.

Table 1. Auto detection Parameters for post-implanted cohorts.

Patient	Shadow Trace min	Shadow Trace max	Stent Search Area min	Stent Search Area max	Stent Intensity
1	0,3	1,0	-0,2	0,1	1,5
2	0,1	1,2	-0,1	0,1	5,2
3	0,3	1,3	-0,2	0,3	4,3
4	0,2	1,0	-0,1	0,3	4,0
5	0,2	1,0	-0,5	0,3	4,0
6	0,3	1,0	-0,1	0,1	4,8

Table 2. Auto detection Parameters for follow-up cohorts.

Patient	Shadow Trace min	Shadow Trace max	Stent Search Area min	Stent Search Area max	Stent Intensity
1	0,1	2,1	-0,2	0,6	1,0
2	0,1	1,5	0,0	0,8	1,0
3	0,1	1,3	0,1	0,7	1,0
4	0,2	1,0	0,0	0,6	3,7
5	0,3	1,0	0,0	0,5	1,0
6	0,2	0,6	0,0	0,4	1,0

Differences in values of Stent Search Area and Stent Intensity parameters between post-implant and follow-up cohorts had been observed. This could be connected to the development of neointima hyperplasia, which causes the stent struts to be incorporated deeper in the vessel tissue. Layer thickness of the new tissue that covered the stent struts could have influenced their peak intensity, hence the brightness of stent strut is dissimilar than after implantation [4].

3.2. Automatic detection efficiency

To investigate the sensitivity of the algorithm, the expert checked pullbacks once more. In case of any visible discrepancy between expert and automated analysis, the data was corrected, i.e. stent struts were added or removed from the initial detection by the expert if needed.

In order to better quantify the efficiency of automated strut detection, factors like precision (P) and sensitivity (S) were defined:

$$P = TP/(TP+FP),$$

$$S = TP/(TP+FN),$$

where:

TP - is a number of true positives stent strut detection (algorithm detected correct stent struts);

FP - is a number of false positive stent strut detection (algorithm did not detect correct stent strut);

FN - is a number of false negative stent strut detection (algorithm detected points, which are not stent struts).

In the post-implanted cohorts (n=6) 5290 struts were detected of which 941 had to be removed and analyst added 976 struts. In the follow-up cohorts (n=6) a total number of detected struts were 4464 of which 1308 had to be removed and 1564 had to be added. The expert review resulted in a precision rate of 82% (post-implanted group) and 67% (follow-up group). Sensitivity rate was 82% (post-implanted group) and in 71% (follow-up group). The summarized data can be found in Table 3 below.

Table 3. Automatic detection efficiency

	Post implanted	Follow-up
Number of detected struts [count]	5290	4464
Number of removed struts [count]	941	1308
Number of added struts [count]	976	1564
Sensitivity [%]	82	71
Precision [%]	82	67

4. Quantitative differences between IVUS and OCT

Measurements were performed for the same vessels using IVUS and OCT imaging methods, what enabled a direct comparison of these two modalities in terms of quantitative assessment. Several parameters are crucial to improve the healing process and behaviour of anatomy of coronary vessel wall and stent placement, like lumen diameter, stent diameter, lumen, stent and vessel area. These parameters were collected from the analysis. In absolute dimensions, stent area were significantly different (using t-test, significance level set at $p < 0.05$) at post-implanted cohort between IVUS and OCT ($8,2 \pm 1,0$ vs. $7,1 \pm 0,7$, respectively), however, the delta change shows almost similar results $2,1 \pm 6,6$ vs. $3,5 \pm 5,8\%$). Considering lumen area, IVUS showed smaller areas at post-implanted cohort and larger at follow-up compared to OCT which resulted in a delta change of $-17,9 \pm 13,8\%$ vs. $-29,7 \pm 15,8\%$, respectively. Tables 4 and 5 show a comparison between data collected by IVUS and OCT methods in both cohorts.

Table 4. Quantitative data obtained by IVUS and OCT in post-implanted cohorts.

	IVUS	OCT	n	p
Stent length [mm]	$17,1 \pm 2,4$	$15,4 \pm 1,6$	6	0,18
Stent area [mm ²]	$8,2 \pm 1,0$	$7,1 \pm 0,7$	6	0,06
Lumen Area [mm ²]	$6,9 \pm 0,8$	$7,6 \pm 0,7$	6	0,16

Table 5. Quantitative data obtained by IVUS and OCT in follow up cohorts.

	IVUS	OCT	n	p
Stent length [mm]	$16,5 \pm 2,5$	$13,9 \pm 0,8$	6	0,04
Stent area [mm ²]	$8,4 \pm 0,7$	$7,4 \pm 0,7$	6	0,04
Lumen Area [mm ²]	$5,7 \pm 1,2$	$5,3 \pm 1,3$	6	0,64

Regarding struts detection, number of struts detected in post-implanted cohorts by IVUS was 322 ± 30 and for OCT $888 \pm 80,0$, while the mean number of individual struts per stent at follow-up was 210 ± 41 in IVUS and 787 ± 41 in OCT. Figure 1 depicts detected struts in the same vessel by two discussed modalities.

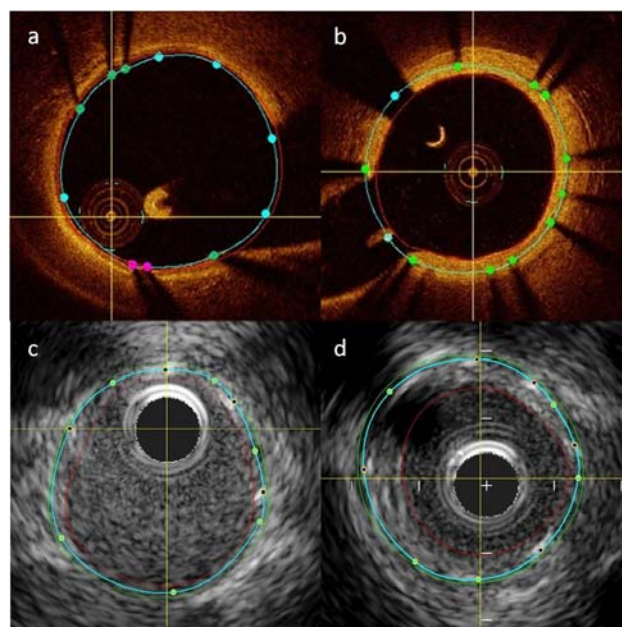


Figure 1. The same cross-section in two modalities
a) OCT post-implanted procedure (green spot - automated detected stent strut , blue spot - control point, pink spot - manually added stent strut;
b) OCT follow-up procedure (green spot - automated detected stent strut , blue spot - control point);

- c) IVUS post-implanted procedure (black spot - manually added stent strut, green spot - control point);
- d) IVUS follow-up procedure (black spot - manually added stent strut, green spot - control point).

5. Results and discussion

Computer-assisted detection of metallic stent struts imaged by OCT presented in the study used the entire pullback data and showed precision and sensitivity of 82% directly after implantation. This score is satisfactory taking into account that previous algorithms had lower precision. The precision and sensitivity score in follow-up cohorts were 67% and 71% respectively, almost 20% higher compared to the precision of previous algorithms. Differences in stent struts detection directly after implantation and during follow up result from OCT method limitation of penetration. Thick layers of tissue covering stent struts change struts peak intensity. Some struts covered by new tissue are showed as bright spots without any trailing shadow, and some struts have only trailing shadow without bright spots.

In recent years several authors presented algorithms used for fully automated detection of metallic stent struts with success score above 90% after implantation and follow up procedure [5-8]. Validation of these algorithms is usually limited to selected number of cross-sections. Mostly good quality images were taken into account, while frames with artifacts were removed from further analysis. For this reason, the efficacy of these algorithms should not be directly compared to the one described in this work, where all frames at previously defined region of interest had been taken into account.

Regarding quantitative analysis, OCT has higher resolution than IVUS which translates into more details being visualized and therefore in a higher number of visible stents struts in comparison to IVUS modality. Stent length also has influence on differences in amount of struts. Another important point to note is that OCT procedures were done without blood in the vessel unlike in IVUS procedure, where sometimes blood speckles make it difficult to distinguish soft plaque from blood. For this reason lumen contour could be less accurate during IVUS analysis.

6. Conclusion

OCT shows considerably more details and quantitative differences of implanted coronary stents as compared to IVUS. This must be taken into account when evaluating new stent platforms using both modalities.

References

- [1] Kang SJ, et al. Tissue characterization of in-sten neointima using intravascular ultrasound radiofrequency data analysis. *Am J Cardiol* 2010; 106: 1561-5.
- [2] Brugaletta S, Costa Jr JR, Garcia-Garcia HM. Assessment of drug-eluting stents and bioresorbable stents by grayscale IVUS and IVUS-based imaging modalities. *Int J Cardiovasc Imaging* 2011; 27: 239-48.
- [3] Suh WM, et al. Intravascular detection of the vulnerable plaque. *Circ Cardiovasc Imaging* 2011; 4: 169-78.
- [4] Bruining N, Sihan K, Ligthart J, De Winter S, Roger E. Automated three-dimensional detection of intracoronary stent struts in optical coherence tomography images. *Computing in Cardiology* 2011.
- [5] Wang A, et al. Automatic stent strut detection in intravascular optical coherence tomographic pullback runs. *Int J Cardiovasc Imaging* 2013; 29: 29-38.
- [6] Ughi GJ, et al. Automatic segmentation of in-vivo intracoronary optical coherence tomography images to assess stent strut apposition and coverage. *Int J Cardiovasc Imaging* 2012; 28: 229-41.
- [7] Lu H, et al. Automatic stent detection in intravascular OCT images using bagged decision trees. *Biomed Opt Express* 2012; 3: 2809-24.
- [8] Bonnema GT, et al. An automatic algorithm for detecting stent endothelialization from volumetric optical coherence tomography datasets. *Phys Med Biol* 2008; 53: 3083-98.

Address for correspondence.

Elzbieta Pociask, MSc
AGH University of Science and Technology
Room C3-203
30 Mickiewicza Av.
30-059 Krakow, Poland
Tel: +48 12-617-50-65
elzbieta.pociask@agh.edu.pl

Klaudia Proniewska, MSc
AGH University of Science and Technology
Room C3-204
30 Mickiewicza Av.
30-059 Krakow, Poland
Tel: +48 12-617-43-70
klaudia.proniewska@agh.edu.pl